TÜBİTAK

Turkish Journal of Chemistry

http://journals.tubitak.gov.tr/chem/

Research Article

Turk J Chem
(2019) 43: 1086 – 1097

doi:10.3906/kim-1902-38

Coumarin-based benzilmonohydrazone as a new proton-sensitive fluorescence dye: synthesis and investigation of photophysical and acidochromic properties

Burcu AYDINER*
Department of Chemistry, Faculty of Science, Gazi University, Ankara, Turkey

Received: 19.02.2019 • **Accepted/Published Online:** 13.05.2019 • **Final Version:** 06.08.2019

Abstract: Coumarin-based chromogenic and fluorogenic dye **4** was designed and synthesized. The photophysical properties of **4** were determined in solvents with different polarities. Protonation affinity was determined by adding trifluoroacetic acid (TFA) to a dichloromethane solution of dye **4** utilizing the UV-Vis and fluorescence titration methods. The protonation region was investigated by using the ^{1}H NMR method. Additionally, DFT and TDDFT studies were performed to support the structural and absorption spectral properties of **4**.

Key words: Coumarin, benzilmonohydrazone, fluorescence dye, acidochromism, proton-sensitive dye

1. Introduction

The design of chromogenic and fluorogenic dye sensors has attracted great attention due to their useful features and functions in many fields such as analytical chemistry, biotechnology, and environmental chemistry [1–4]. Because of the rapid response time, easy visual detection, high sensitivity, and ease of use, these chemosensors have become more appealing than any spectroscopic methods [5]. Chromogenic and fluorogenic sensors are compounds that show changes in color and emission when a guest molecule interacts with the receptor. The design of these chemosensors is based on a chromophore/fluorophore and suitable receptor for the selected analyte [6,7]. One of the important classes of chemosensors includes the proton-sensitive dyes. They have been used in rewritable papers; for the determination of pH changes inside living cells, which is important for tracking biological process dye-sensitized solar cells (DSSCs); and for the determination of photostability of textile dyes [8–11].

Heterocyclic compounds bearing coumarin moiety are among the well-known chromophore groups for important chromogenic/fluorogenic sensors [12]. Coumarins that are substituted at the 7-position with a diethylamino group are especially well known for their applications in chemosensor chemistry, laser dyes, fluorescent markers for amino acids, anions/cations, organic light-emitting diodes, and sensitizers in DSSCs as chromogenic and fluorochromogenic chromophores [13–17].

When the electron-donating group is at the 7-position of the coumarin ring, the absorption maxima of the compound shift to red due to the intramolecular charge transfer (ICT) from the amino group to lactone carbonyl [18]. The bathochromic shift will increase if there is an electron-accepting group at the 3-position of coumarin [19]. By changing the accepting groups at the 3-position, a range of chromogenic and fluorogenic chemosensors with a variety of photophysical properties can be obtained [20]. In this study, benzilmonohydrazone dye-

*Correspondence: baydiner@gazi.edu.tr

appended coumarin (**4**) was synthesized under mild reaction conditions, as shown in Scheme 1, and investigated for its solvatochromic effects with solvents of different polarity. The chemosensor properties of **4** were then investigated by using absorption, emission, and ^{1}H NMR spectroscopic methods in an acidic environment using trifluoroacetic acid (TFA). Moreover, geometry optimization of **4** was carried out and TDDFT studies were also performed to explain some photophysical properties of **4** in different solvents.

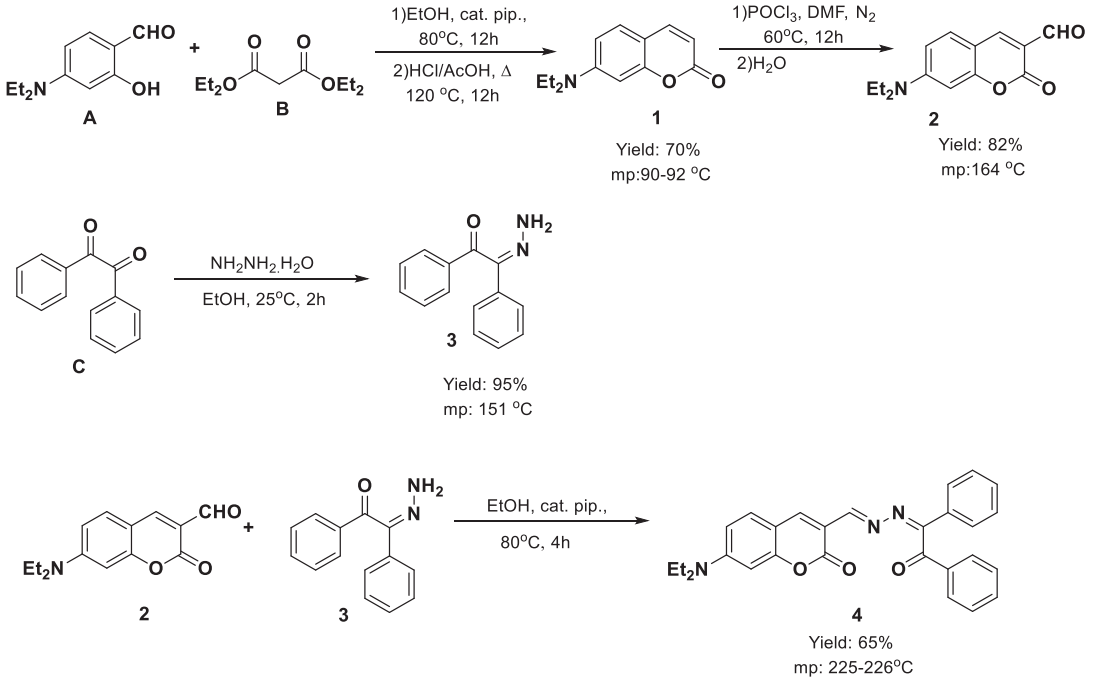

Scheme 1. The synthetic pathways of synthesis of chemosensor **4**.

2. Experimental

2.1. General

All commercially available chemicals were of reagent grade and used without further purification. Thin-layer chromatography (TLC) was used for monitoring the reactions using precoated silica gel 60 F254 plates. Column chromatography was performed on silica gel (60-120 mesh, Merck Chemicals). NMR spectra were measured on Bruker Avance 300 (^{1}H: 300 MHz, ^{13}C: 75 MHz) spectrometers at 20 °C (293 K). Chemical shifts (δ) are given in parts per million (ppm) using the residue solvent peaks as a reference relative to TMS. Coupling constants (J) are given in hertz (Hz). Signals are abbreviated as follows: singlet, s; doublet, d; doublet-doublet, dd; triplet, t; multiplet, m. High-resolution mass spectra (HR-MS) were recorded at the Gazi University Faculty of Pharmacy using electron ionization (EI) mass spectrometry Waters-LCT-Premier-XE-LTOF (TOF-MS) instruments in m/z (rel. %). The melting points were measured using an Electrothermal IA9200 apparatus. Absorption spectra were recorded on a Shimadzu 1800 spectrophotometer; fluorescence spectra were recorded on a Hitachi F-7000 fluorescence spectrophotometer.

2.2. Synthesis of 7-(diethylamino)coumarin-3-aldehyde (2)

Compound **2** was synthesized as reported earlier [20]. The first step was the synthesis of 7-(diethylamine)-2H-chromene-2-one (**1**) by using diethylaminosalicylaldehyde (A) and diethylmalonate (B) with piperidine as a

catalyst and also AcOH and concentrated HCl as decarboxylating agents. The second step was the formylation of compound **1** at the 3-position of coumarin using Vilsmeier Haack reagent ($POCl_3$ and DMF) in an inert atmosphere. Yield: 82%; mp: 164 °C (lit.: 168–170 °C); ^{1}H NMR (300 MHz, $CDCl_3$)δ 9.90 (s, 1H), 7.64 (d, J = 9.1, 1H), 6.85 (dd, J = 9.19 and 2.4 Hz, 1H), 6.61 (d, J = 2.3, 1H), 3.51 (q, J = 7.1, 4H), 1.17 (d, J = 7.0, 6H).

2.3. Synthesis of benzilmonohydrazone (3)

Compound **3** was synthesized by simple condensation between benzil (C) and hydrazine hydrate in ethanol utilizing a reported method [21]. Yield: 95%; mp: 151 °C (lit.: 151 °C)

2.4. Synthesis of 7-(diethylamino)-3-((*E*)-(((*E*)-2-oxo-1,2-diphenylethylidene)hydrazono)methyl)-2*H*-chromen-2-one (4)

Compound **4** was synthesized by mixing 7-(diethylamino)coumarin-3-aldehyde (**2**) (1 mmol, 245 mg) with benzilmonohydrazone (**3**) (1 mmol, 224 mg) in 20 mL of ethanol and three drops of acetic acid. The mixture was refluxed for 4 h, then cooled and filtered, and the dark orange solid was washed with ethanol. It was used without any purification process. Yield: 65%; mp: 225–226 °C. FT-IR (ATR, ν_{max}, cm^{-1}): 3063 (Ar-H); 2972 (R-H); 1713 (C=O); 1673 (C=O); 1615 (C=N). ^{1}H-NMR (300 MHz, $CDCl_3$) δ 8.79 (s, 1H), 7.95 (dd, J = 8.9 and 2.4 Hz, 2H), 7.86 (s, 1H), 7.83 (dd, J = 8.3 and 1.7 Hz, 2H), 7.63–7.34 (m, 6H), 7.15 (d, J = 8.9 Hz, 1H), 6.53 (dd, J = 8.9 and 2.4 Hz, 1H), 6.43 (d, J = 2.3 Hz, 1H), 3.42 (q, J = 7.1 Hz, 4H), 1.24 (t, J = 7.2 Hz, 6H) (Figure 1). ^{13}C-APT (75 MHz, $CDCl_3$): δ 197.9; 166.3; 161.5; 157.6; 157.3; 151.9; 141.4; 135.6; 133.8; 132.7; 131.3; 130.8; 129.2; 128.9; 128.8; 127.7; 112.8; 109.4; 108.6; 97.1; 45.0; 12.4 (Figure 2). HR-MS (m/e) $(M-H)^+$: $C_{28}H_{26}N_3O_3$, calc.: 452.1974 ; found: 452.1983, [δm/m (ppm) = 1.99].

3. Results and discussion

3.1. Synthesis

Compound **4** was synthesized by the stepwise procedure demonstrated in Scheme 1. The reaction of 7-(diethylamino)coumarin-3-aldehyde (**2**) with benzilmonohydrazone (**3**) in the presence of piperidine gave 7-(diethylamino)-3-((*E*)-(((*E*)-2-oxo-1,2-diphenylethylidene)hydrazono)methyl)-2*H*-chromen-2-one (**4**). The structure of the compound was confirmed by FT-IR, ^{1}H NMR, ^{13}C-APT NMR, and HR-MS techniques. The compound was obtained with moderate yield (65%).

3.2. Photophysical properties

The UV-Vis spectral data of dye **4** were measured in different solvents with various polarities at room temperature. Compound **4** is soluble in tetrahydrofuran (THF), dichloromethane (DCM), chloroform (Chl), and dimethyl sulfoxide (DMSO), while it is sparingly soluble in protic polar solvents such as acetic acid (AcOH), methanol (MeOH), and ethanol (EtOH) at 10 μM. Effects of solvent polarity on absorption and emission spectra of the chemosensor were investigated and photographs of the color changes were taken under daylight and UV light. The absorption coefficients (ε) were calculated according to the Beer–Lambert law and values are given in Table 1. In Figure 3, normalized absorption and emission spectra of **4** in four selected solvents (THF, DCM, Chl, and DMSO) can be seen. Chemosensor **4** showed red-shifted absorption with an increase in solvent polarity

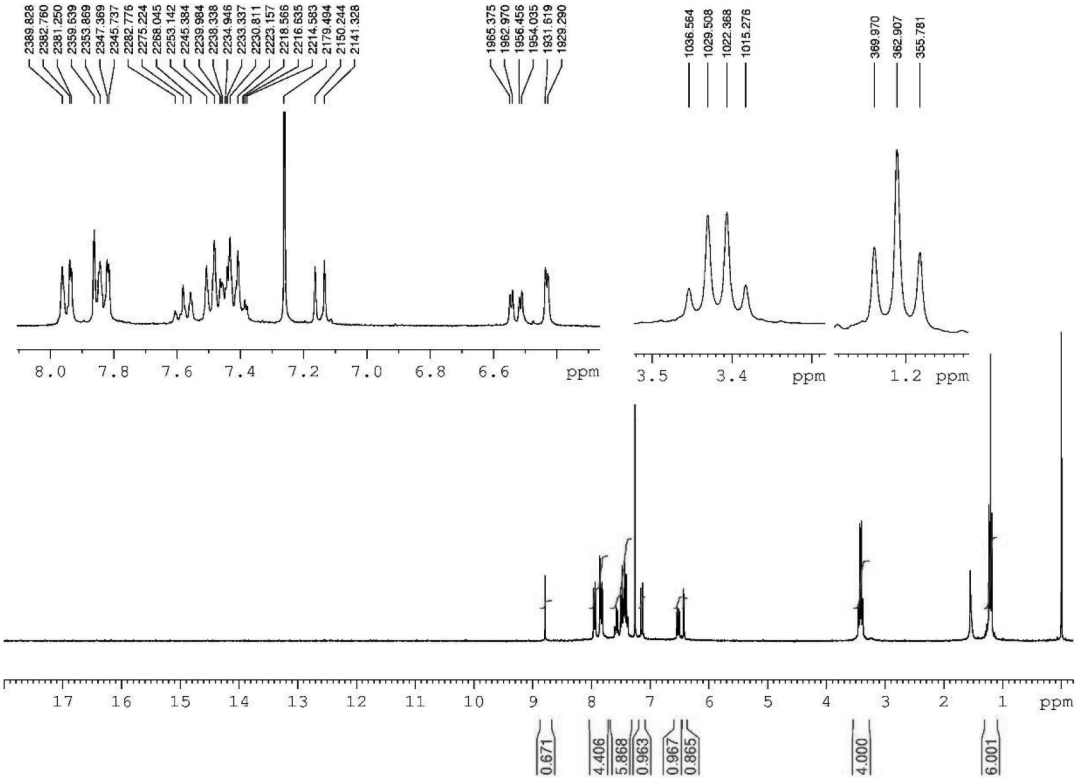

Figure 1. ^{1}H NMR spectra of **4**.

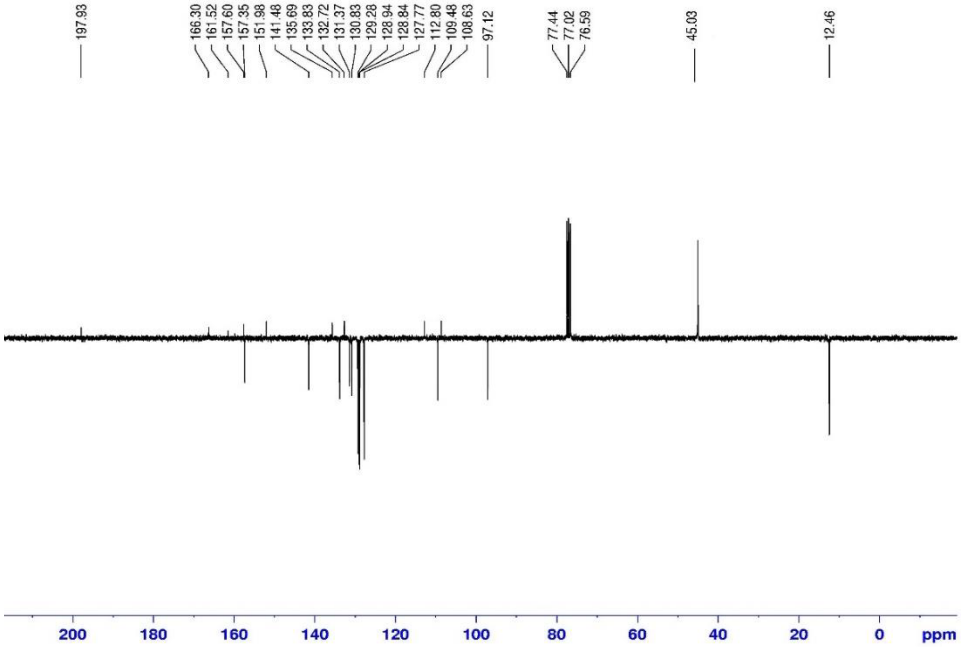

Figure 2. ^{13}C-APT NMR spectra of **4**.

(THF to DMSO), except for Chl. Similar to the absorption spectra, emission maxima were red-shifted with increased solvent polarity. There was a high maxima difference (24 nm) between DMSO and the other three solvents. This significant difference between DMSO and the other solvents was caused by solvent polarity. The 7-diethylamino-substituted coumarin compound has fluorescence properties due to ICT from the dialkylamino group to lactone carbonyl. When the polarity of solvents change, different absorption and emission behaviors can be seen. This behavior of the 7-dialkylaminocoumarin dyes in high-polarity solvents like DMSO is considered to be due to the formation of their twisted intramolecular charge transfer states and the consequent enhancement in the nonradiative decay channel for the excited dyes [22,23]. Although 7-diethylaminocoumarins are well-known fluorescence dyes because of their high fluorescence properties, the fluorescence intensity of **4** is very low. Hydrazone-based fluorescent dyes can be capable of undergoing reversible changes of configuration, and E/Z isomerization can occur by rotation and inversion in the C=N bond. These processes can be caused by photoisomerism and result in the rotation of the substituents around the C=N double bond, which can cause a change in the transition state of molecules. This process can definitely be a reason for their low fluorescence properties [24,25].

Table 1. Photophysical properties of chemosensor **4** in various solvents.

Solvents	$\lambda^{a}_{abs-max}$ (nm)	λ^{b}_{fl-max} (nm)	ε^{c} (λ_{max})
THF	465	482	63300
DCM	468	482	49900
Chl	463	480	64500
DMSO	479	504	46100

[a]Long wavelength absorption maximum, in nm; c = 10 μM; [b]emission maximum, in nm; c = 10 μM [c]ε= molar absorption coefficient, cm^{-1} M^{-1}.

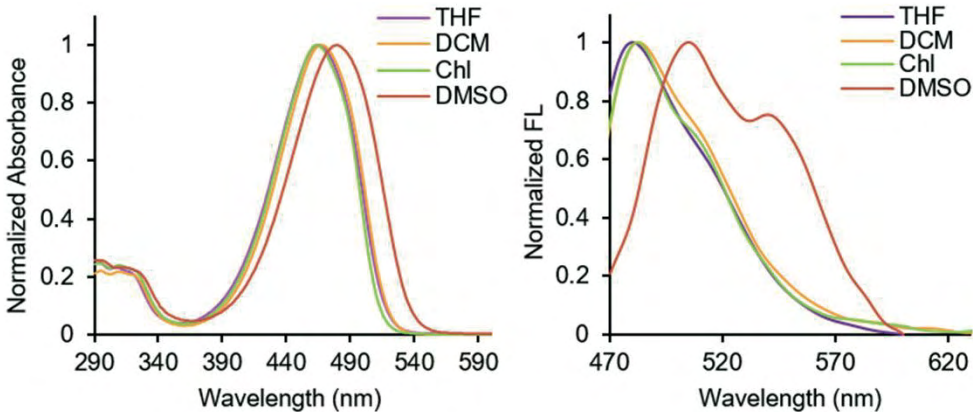

Figure 3. Normalized absorption and emission spectra of **4** in different solvents (c = 10 μM, λ_{abs} values in Table 1 were used for each solvent as λ_{ex}).

The absorption and emission color changes of the chemosensor were also investigated and the photographs can be seen in Figure 4. Under ambient light, the absorption color of **4** changed from yellow to orange when solvent polarity increased to an aprotic polar solvent (DMSO). While the dye has very low intensity, it showed green emission in THF, DCM, and Chl and orange in DMSO under UV light ($\lambda_{ex.}$ = 365 nm).

Figure 4. The color of **4** in various solvents under ambient light (left) and UV light (right) ($\lambda_{ex.}$ = 365 nm), c= 10 μM.

3.3. Acidochromic properties

Determination of the pH changes with a fast and easy method, such as color changes with increased/decreased acidic and basic species in media, has attracted considerable attention recently. For that purpose, the acidochromic behavior of chemosensor **4** was investigated in the presence of TFA in DCM. The change in the absorption and emission spectra of **4** upon addition of TFA is illustrated in Figure 5. The chemosensor exhibits significant acidochromic properties. Upon the addition of increased TFA, the absorption maxima shifted from 468 nm to 542 nm and a well-defined isosbestic point at 490 nm was observed. This large shift (72 nm) in absorption maxima can arise from the protonation of lactone carbonyl or hydrazone nitrogens due to increased ICT [15,26]. In our previous studies, we tested the acidochromic properties of a series of coumarin-based functional dyes bearing diethylamino at the 7-position of coumarin and a bathochromic shift in acidic medium was seen because of the obtained ICT between the diethylamino and protonated groups attached at the 3-position of coumarin. Therefore, if there was protonation in the diethylamino group, hypsochromic shifts of absorption would be expected. Possible protonated forms of **4** are given in Scheme 2.

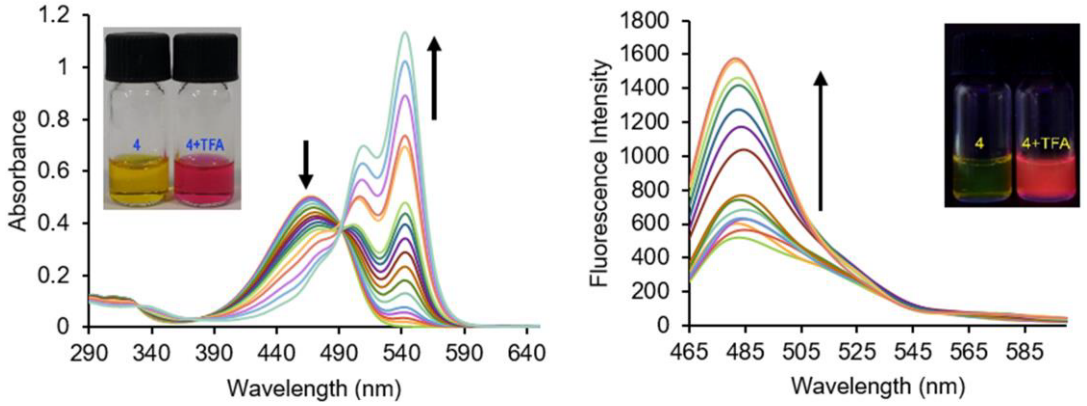

Figure 5. Spectrophotometric titrations of **4** (c= 10 μM, λ_{ex} = 468 nm) in DCM upon addition TFA (c= 10 mM). Insets: Pictures of the color (left) and emission (right) changes in DCM solutions of compound **4** (c = 10 μM in the presence of TFA).

Emission spectra of **4** was also investigated in the presence of TFA, as shown in Figure 5. Upon the addition of TFA, the emission intensity of **4** began to increase. This increased fluorescence intensity can be explained by an enhancement of ICT in the molecule from the 7-diethylamino part to the lactone carbonyl or hydrazone group by protonation [26].

Similar to the UV-Vis and fluorimeter titration results, upon the addition of TFA to **4**, a significant color

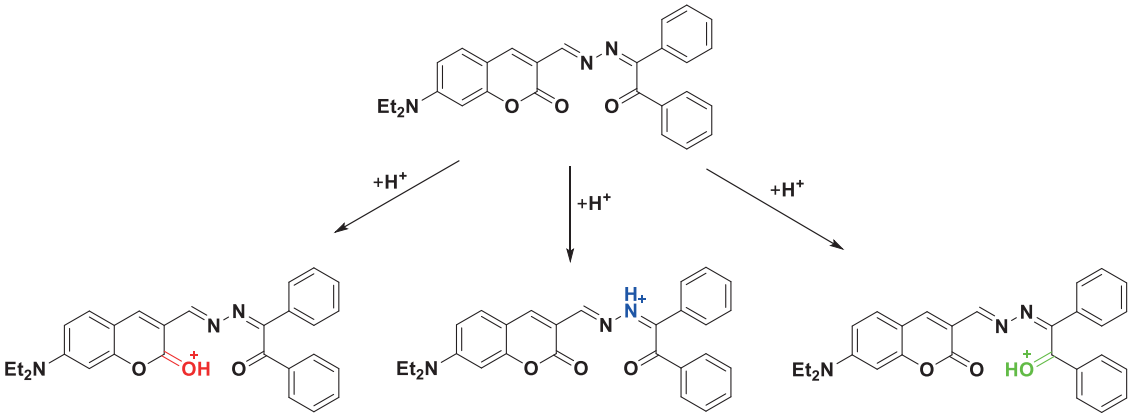

Scheme 2.The possible protonation regions of the dye.

change was observed from yellow to dark pink in daylight, as well as increased pink fluorescence intensity under UV light, as shown in Figure 5 (insets).

To examine the potential application of compound **4** as a chemosensor in more complicated environments, various metal ions of biological and environmental interest including K^+, Ca^{2+}, Mg^{2+}, Cd^{2+}, Cu^{2+}, Zn^{2+}, Ni^{2+}, Hg^{2+}, Co^{2+}, Sn^{2+}, Pb^{2+}, Al^{3+}, and Fe^{3+} were also investigated and, as can be seen in Figure 6, no change in absorption maxima was found.

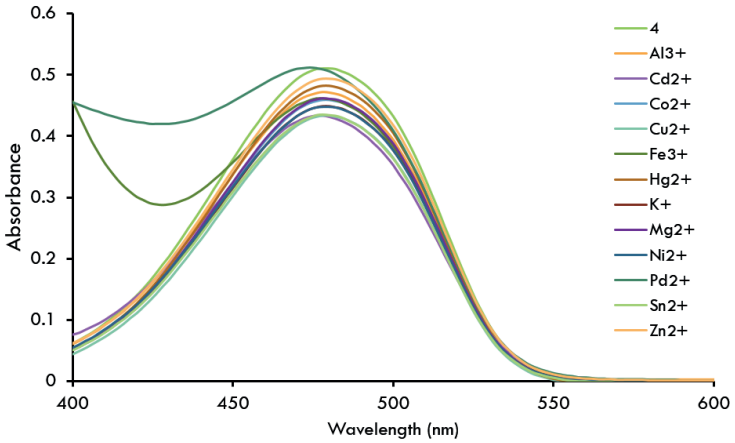

Figure 6. Absorption spectra of **4** (c= 10 μM) in DMSO upon the addition of 100 equiv. various cations (c= 10 mM).

3.4. NMR studies

To determine the protonation region in compound **4** after the addition of TFA, ^{1}H NMR and COSY spectra were taken as shown in Figures 7 and 8, respectively. While a significant shift of the signals of **4** is observed from coumarin protons after the addition of TFA, there was no change at the imine proton ($\mathbf{H_1}$) at 8.79 ppm and protons at the phenyl rings slightly shifted. Coumarin hydrogens $\mathbf{H_2}$, $\mathbf{H_3}$, $\mathbf{H_4}$, and $\mathbf{H_5}$ shifted to the upper field due to the decreased electron density in the ring system (from δ 7.86, 7.15, 6.53, and 6.44 to δ 8.35, 7.63, 6.87, and 6.50, respectively; see Table 2 for values). COSY spectra helped to determine the exact position of the $\mathbf{H_3}$ signal that shifted to the upper field. This showed that only coumarin protons shifted significantly and

protonation mainly affected the coumarin ring. The results of NMR study indicate that the coumarin lactone was protonated.

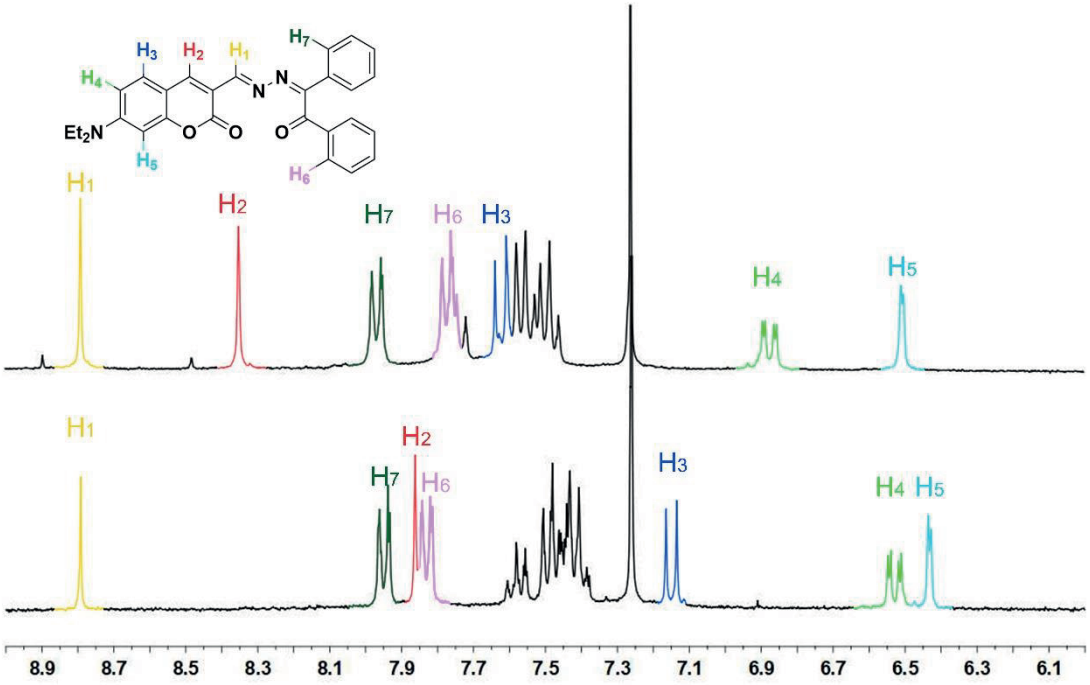

Figure 7. Partial ^{1}H NMR spectra of chemosensor **4** (bottom) and upon the addition of TFA (top).

Table 2. Chemical shift values of **4** and after adding TFA.

	4 (ppm)	**4** + TFA (ppm)	$\Delta\delta^a$
$\mathbf{H_1}$	8.79	8.79	-^{b}
$\mathbf{H_2}$	7.86	8.35	+0.51
$\mathbf{H_3}$	7.15	7.63	–0.43
$\mathbf{H_4}$	6.53	6.87	–0.34
$\mathbf{H_5}$	6.44	6.50	+0.14
$\mathbf{H_6}$	7.83	7.76	+0.13
$\mathbf{H_7}$	7.95	7.95	^{b}

^{a}(+) indicates upper field shift, (–) indicates lower field shift; ^{b} no change observed.

3.5. Theoretical studies

The possible conformations of **4** were obtained with PES scans around torsion angles τ_1 = C10-N20-C21-C22 and τ_2 = C10-N20-C28-C29 using the HF method and the 6-31G basis set. The most stable conformation of the compound was obtained using the B3LYP method at the 6-31+G(d,p) basis set in gas phase as seen in Figure 9. The selected bond lengths (Å), angles (°), and torsion angles (°) of **4** are given in Table 3. After that, polarizable continuum model (PCM) calculations were carried out in four different solvents (THF, DCM, Chl, and DMSO) [27]. Finally, time-dependent density functional theory (TDDFT) calculations were performed

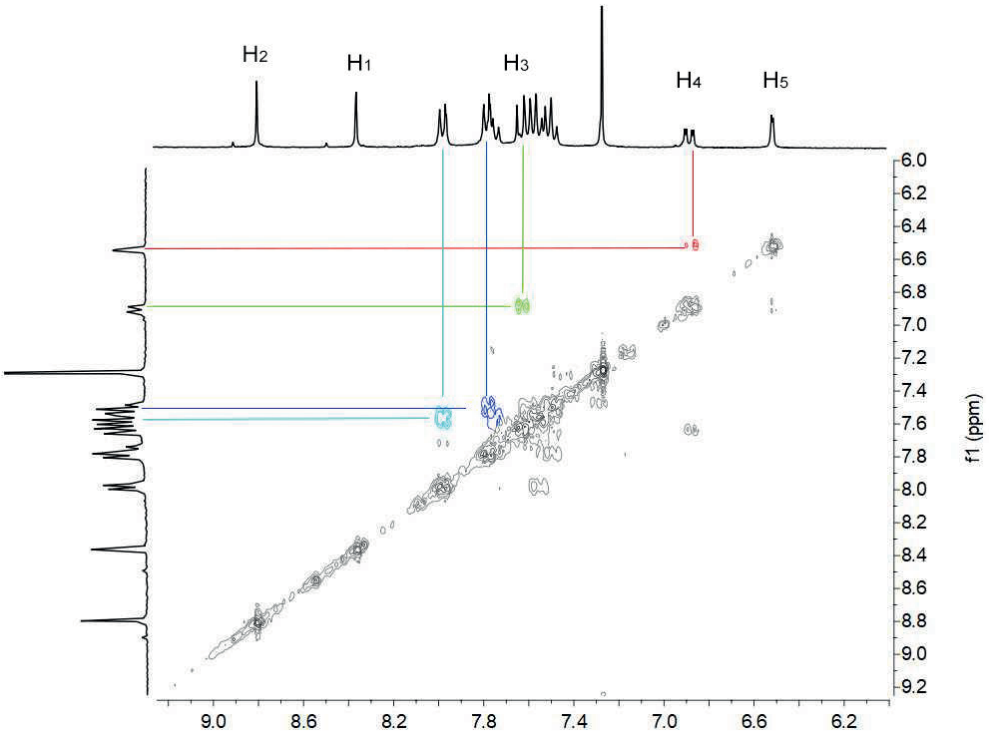

Figure 8. COSY spectra of chemosensor **4** upon the addition of TFA.

at B3LYP/6-31+G(d,p) level to obtain the absorption spectra, singlet vertical excitation energies, oscillator strengths, and percentages of major contributions of the calculated transitions using the optimized structures (Table 4) [28]. Vibrational frequencies were calculated to make sure no imaginary frequency existed for the structures. All calculations were carried out with the Gaussian 09 program package [29].

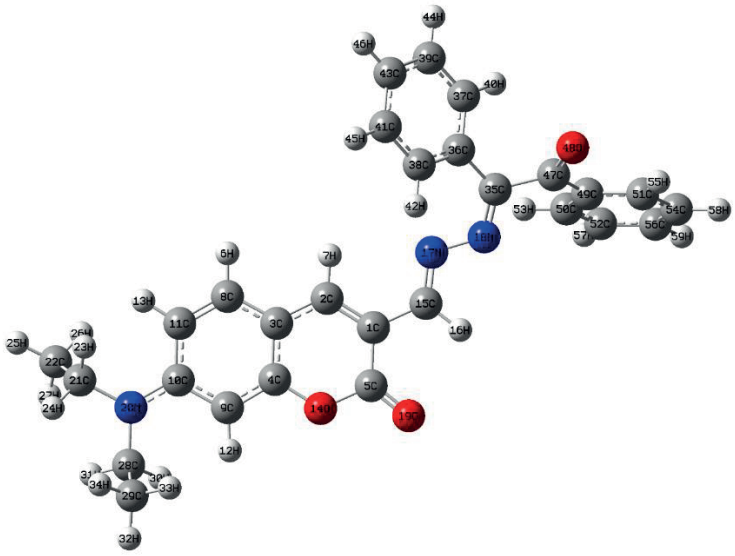

Figure 9. The optimized geometry of **4** with atomic numbering in gas phase.

Table 3. Selected bond lengths (Å), angles (°), and the torsion angles (°) of **4**.

Parameter	B3LYP	Parameter	B3LYP
Bond lengths		Bond angles	
C47–C49	1.496	O48–C47–C49	120.8
C47–C35	1.519	N18–C35–C36	127.9
C47–O48	1.227	N17–N18–C35	117.1
N18–C35	1.296	C10–N20–C28	121.8
N17–N18	1.378	C21–N20–C28	116.0
N17–C15	1.294	Torsion angles	
C5–O19	1.212	N17–N18–C35–C36	4.5
C5–O14	1.398	C15–N17–N18–C35	–158.6
N20–C10	1.374	C5–C1–C15–N17	178.9
N20–C21	1.465	C28–N20–C10–C11	174.0

Table 4. The experimental and calculated λ_{max} values of **4**.

Solvent	λ_{max} exp.(nm)	λ_{max} calc.(nm)	Oscillator strength	E (eV)	Major contribution
THF	465	494	1.0241	2.5094	HOMO/LUMO (95%)
DCM	468	496	1.0332	2.5005	HOMO/LUMO (95%)
Chl	463	491	1.0220	2.5234	HOMO/LUMO (95%)
DMSO	479	501	1.0427	2.4752	HOMO/LUMO (96%)

All the maximum absorption wavelengths are mainly due to n-π^* transitions and the computed absorption maxima were found to be 22–29 nm larger than the experimental ones. The chemosensor absorbs at the highest wavelength (501 nm) with the oscillator strength of 1.0427 in DMSO. This is due to 96% contributions from HOMO/LUMO. The maximum absorption wavelengths in all of the other solvents are due to 95% contributions from HOMO/LUMO.

The increase in λ_{max} is similar to the changes in solvent polarity both experimentally and theoretically. The lowest λ_{max} values, which were in chloroform (exp.: 463 nm, calc.: 491 nm), and the highest ones, which were in DMSO (exp.:479 nm, calc.: 501 nm), were compatible with experimental absorption maxima.

3.6. Conclusions

In conclusion, a novel coumarin-benzilmonohydrazone-based colorimetric and turn-on fluorescence acid-sensitive dye was synthesized. The results showed that both absorption and emission values shifted to the bathochromic region with the addition of TFA. Significant colorimetric and fluorometric color changes were also observed with an increase in the environment's acidity. This behavior indicates that **4** can be used as a proton-sensitive chemosensor.

Acknowledgment

I would like to thank Assoc Prof Dr Ebru Aktan for her support in the theoretical studies.

References

1. Santos-Figueroa LE, Moragues ME, Climent E, Agostini A, Martínez-Man ez R et al. Chromogenic and fluorogenic chemosensors and reagents for anions. A comprehensive review of the years 2010–2011. Chemical Society Reviews 2013; 42: 3489-3613. doi: 10.1039/C3CS35429F
2. Klymchenko AS. Solvatochromic and fluorogenic dyes as environment-sensitive probes: design and biological applications. Accounts of Chemical Research 2017; 50 (2): 366-375. doi: 10.1021/acs.accounts.6b00517
3. Guo Z, Zhu W, Tian H. Dicyanomethylene-4H-pyran chromophores for OLED emitters, logic gates and optical chemosensors. Chemical Communications 2012; 48 (49): 6073-6084. doi: 10.1039/C2CC31581E
4. Kim TI, Hwang B, Bouffard J, Kim Y. Instantaneous colorimetric and fluorogenic detection of phosgene with a *meso*-oxime-BODIPY. Analytical Chemistry 2017; 89 (23): 12837-12842. doi: 10.1021/acs.analchem.7b03316
5. Liu XD, Xu Y, Sun R, Xu YJ, Lu JM et al. A coumarin–indole-based near-infrared ratiometric pH probe for intracellular fluorescence imaging. Analyst 2013; 138 (21): 6542-6550. doi: 10.1039/C3AN01033C
6. Li X, Gao X, Shi W, Ma H. Design strategies for water-soluble small molecular chromogenic and fluorogenic probes. Chemical Reviews 2014; 114: 590-659. doi: 10.1021/cr300508p
7. Shao J, Lin H, Lin H. Rational design of a colorimetric and ratiometric fluorescent chemosensor based on intramolecular charge transfer (ICT). Talanta 2008: 77 (1): 273-277. doi: 10.1016/j.talanta.2008.06.035
8. Zhang T, Sheng L, Liu J, Ju L, Li J et al. Photoinduced proton transfer between photoacid and pH-sensitive dyes: influence factors and application for visible-light-responsive rewritable paper. Advanced Functional Materials 2018; 28 (16): 1705532. doi: 10.1002/adfm.201705532
9. Han JY, Burgess K. Fluorescent indicators for intracellular pH. Chemical Reviews 2010; 110: 2709-2728. doi: 10.1021/cr900249z
10. Teoli F, Lucioli S, Nota P, Frattarelli A, Matteocci F et al. Role of pH and pigment concentration for natural dye-sensitized solar cells treated with anthocyanin extracts of common fruits. Journal of Photochemistry and Photobiology A: Chemistry 2016; 316: 24-30. doi: 10.1016/j.jphotochem.2015.10.009
11. Plutino MR, Guido E, Colleoni C, Rosace G. Effect of GPTMS functionalization on the improvement of the pH-sensitive methyl red photostability. Sensors and Actuators B: Chemical 2017; 238: 281-291. doi: 10.1016/j.snb.2016.07.050
12. Li H, Cai L, Chen Z. Advances in Chemical Sensors. Rijeka, Croatia: InTech, 2012.
13. Goswami S, Das AK, Maity S. 'PET' vs. 'push–pull' induced ICT: a remarkable coumarinyl-appended pyrimidine based naked eye colorimetric and fluorimetric sensor for the detection of Hg^{2+} ions in aqueous media with test trips. Dalton Transactions 2013; 42 (46): 16259-16263. doi: 10.1039/C3DT52252K
14. Babür B, Seferoğlu N, Öcal M, Sonugur G, Akbulut H et al. A novel fluorescence turn-on coumarin-pyrazolone based monomethine probe for biothiol detection. Tetrahedron 2016; 72 (30): 4498-4502. doi: 10.1016/j.tet.2016.06.008
15. Aydıner B, Seferoğlu Z. Proton sensitive functional organic fluorescent dyes based on coumarin-imidazo[1,2-*a*]pyrimidine; syntheses, photophysical properties, and investigation of protonation ability. European Journal of Organic Chemistry 2018; 43: 5921-5934?. doi: 10.1002/ejoc.201800594
16. Chemchem M, Yahaya I, Aydıner B, Seferoğlu N, Doluca O et al. A novel and synthetically facile coumarin-thiophene-derived Schiff base for selective fluorescent detection of cyanide anions in aqueous solution: synthesis, anion interactions, theoretical study and DNA-binding properties. Tetrahedron 2018; 76 (48): 6897-6906. doi: 10.1016/j.tet.2018.10.008

17. Chen Q, Wu N, Liu Y, Li X, Liu B. Twisted coumarin dyes for dye-sensitized solar cells with high photovoltage: adjustment of optical, electrochemical, and photovoltaic properties by the molecular structure. RSC Advances 2016; 6 (91): 87969-87977.

18. Liu X, Cole J M, Waddell PG, Lin TC, Radia J et al. Molecular origins of optoelectronic properties in coumarin dyes: toward designer solar cell and laser applications. Journal of Physical Chemistry A 2011; 116 (1): 727-737. doi: 10.1039/C6RA17930D

19. Demchenko AP. Introduction to Fluorescence Sensing. Berlin, Germany: Springer Science & Business Media, 2008.

20. Sheng R, Wang P, Liu W, Wu X, Wu S. A new colorimetric chemosensor for Hg^{2+} based on coumarin azine derivative. Sensors and Actuators B: Chemical 2008; 128 (2): 507-511. doi: 10.1016/j.snb.2007.07.069

21. Wieland M, Seichter W, Schwarzer A, Weber E. Influence of different aryl substitution on the crystal structures of benzil monohydrazone and dibenzil azine parent compounds. Structural Chemistry 2011; 22 (6): 1267. doi: 10.1007/s11224-011-9817-9

22. Raju BB, Varadarajan TS. Substituent and solvent effects on the twisted intramolecular charge transfer of three new 7-(diethylamino)coumarin-3-aldehyde derivatives. Journal of Physical Chemistry 1994; 98: 8903-8905. doi: 10.1021/j100087a014.

23. Satpati AK, Kumbhakar M, Nath S, Pal H. Photophysical properties of coumarin-7 dye: Role of twisted intramolecular charge transfer state in high polarity protic solvents. Photochemistry and Photobiology 2009; 85: 119-129. doi: 10.1111/j.1751-1097.2008.00405.x.

24. Yoshino J, Kano N, Kawashima T. Fluorescent azobenzenes and aromatic aldimines featuring an N–B interaction. Dalton Transactions 2013; 42 (45): 15826-15834. doi: 10.1039/C3DT51689J

25. Romero EL, D'Vries RF, Zuluaga F, Chaur MN. Multiple dynamics of hydrazone based compounds. Journal of the Brazilian Chemical Society 2015; 26 (6): 1265-1273. doi: 10.5935/0103-5053.20150092

26. Liu X, Cole JM, Waddell PG, Lin TC, Radia J et al. Molecular origins of optoelectronic properties in coumarin dyes: toward designer solar cell and laser applications. Journal of Physical Chemistry A 2012; 116: 727-737. doi: 10.1021/jp209925y.

27. Cossi M, Barone V, Cammi R, Tomasi J. Ab initio study of solvated molecules: a new implementation of the polarizable continuum model. Chemical Physics Letters 1996; 225: 327-335. doi: 10.1016/0009-2614(96)00349-1

28. Adamo C, Jacquemin D. The calculations of excited-state properties with time-dependent density functional theory. Chemical Society Reviews 2013; 42: 845-856. doi: 10.1039/C2CS35394F

29. Frisc MJ, Trucks GW, Schlegel HB, Scuseria GE, Robb MA et al. Gaussian 09 (Revision C.01). Wallingford, CT, USA: Gaussian Inc., 2010.